Zema, Sebastiano Michele

Working Paper

Uncovering the network structure of non-centrally cleared derivative markets: Evidences from regulatory data

ECB Working Paper, No. 2721

Provided in Cooperation with:
European Central Bank (ECB)

Suggested Citation: Zema, Sebastiano Michele (2022) : Uncovering the network structure of non-centrally cleared derivative markets: Evidences from regulatory data, ECB Working Paper, No. 2721, ISBN 978-92-899-5308-5, European Central Bank (ECB), Frankfurt a. M., https://doi.org/10.2866/808285

This Version is available at:
https://hdl.handle.net/10419/269128

EUROPEAN CENTRAL BANK
EUROSYSTEM

Working Paper Series

Sebastiano Michele Zema

Uncovering the network structure of non-centrally cleared derivative markets: evidences from regulatory data

No 2721 / September 2022

Abstract

The network structure of non-centrally cleared derivative markets, uncovered via the European Market Infrastructure Regulation (EMIR), is investigated with a focus on the Covid-19 market turmoil period. Initial and variation margin networks are reconstructed to analyze channels of potential losses and liquidity dynamics. Despite the absence of central clearing, the derivative network is found to be ultrasmall and a filtering tool is proposed to identify channels in the network characterized by the highest exposures. I find these exposures to be mainly toward institutions outside the euro-area (EA), emphasizing the need for cooperation across different jurisdictions. Anomalous behavior in terms of diverging first and second moments on the degree and strength distributions are detected, signaling the presence of large exposures generating extreme liquidity outflows. A reference table of parameters' estimates based on real data is provided for different network sizes, with no break of confidentiality, making possible to simulate in a realistic way the liquidity dynamic in global derivative markets even when the access to supervisory data is not granted.

JEL codes: G01, G15, G23.

Keywords: Financial derivatives, non-centrally cleared exposures, complex networks, maximum spanning trees, fat-tails.

Non-technical summary

Non-centrally cleared derivative transactions can embed substantial risks, which might not be adequately monitored given the absence of central clearing counterparties, as proven by the recent default of Archegos Capital Management in March 2021. By using the voluminous transaction-by-transaction data collected under the European Market Infrastructure Regulation, this paper shed lights on bilateral derivative transactions that have not been centrally cleared through CCPs.

Two types of collateralization networks will be uncovered, namely the initial and the variation margin networks. The initial margins represent the riskiness of the exposures in terms of future potential losses, while the variation margins are used to compensate daily fluctuations in the market value of the derivative contract and can expose counterparties to severe liquidity outflows. The two networks are very large and hard to analyze, requiring the implementation of ad-hoc filtering procedures and methodologies finding their roots in the network science literature. After analyzing the network of non-centrally cleared exposures and its structural properties, a filtering tool for monitoring purposes will be addressed. Finally, a robust statistical description for the shape of the distributions associated to the two networks will be provided.

Two main findings will be highlighted in the paper. First, the channels containing the highest exposures, and identified through the proposed filtering tool, involve mainly institutions belonging to jurisdictions outside the euro area (EA). Second, both initial and variation margin networks display anomalous behaviors in the power-law parameter associated respectively to both the degree and in/out-strength distributions, signaling the presence of extreme positions and liquidity outflows during turmoil periods to be brought to the attention of policy makers and supervisory authorities.

1 Introduction

The recent default of Archegos Capital Management in March 2021, caused by exposures on Total Return Swaps (TRS) on equities and combined with the adoption of poor margining practices, signaled how appropriate risk mitigation techniques and supervision must take place even when derivative contracts are not centrally cleared by central clearing counterparties (CCPs). According to the latest statistical release from the Bank of International Settlements (BIS) on OTC derivatives statistics, central clearing rates for interest rate derivatives (IRDs) and credit default swaps (CDS) stand respectively at 78% and 62% of total notional at the end 2021[1]. Moreover, some types of equity derivative instruments as Contract for Differences (CFD) and Total Return Swaps (TRS) are mostly exchanged bilaterally among counterparties with no central clearing in place[2].

This paper sheds lights on bilateral derivative transactions that have not been centrally cleared through CCPs by using the voluminous transaction-by-transaction data collected under the European Market Infrastructure Regulation ('EMIR data'). The collateral network structure of non-centrally cleared derivative markets is uncovered, analyzing the implications of the detected structures from a systemic risk and monitoring perspectives. The implementation of a filtering tool to extract relevant information from such large and complex networks will be proposed, also providing the literature with robust parameters' estimates to promote the adoption of appropriate distributional assumptions for the modeling of such networks. This will allow other researchers, with no access to this kind of confidential data, to simulate and replicate the structure of derivative markets in a realistic way.

In the aftermath of the 2008 Global Financial Crisis the weaknesses of derivatives markets and the necessity to increase their transparency become evident to the regulators. Despite the important role played by financial derivatives in the economy, these instruments embed substantial risks which were significant drivers of the collapse of Lehman Brothers and the near-failure of AIG (McDonald and Paulson, 2015). To this end, the G20 leaders decided at the 2009 summit in Pittsburg to make over the counter (OTC) derivatives trading safer and more transparent.

In Europe, to implement these goals, the initiative was formalized in 2012 in the European

[1]Statistical release from the BIS website available at Statistical release: OTC derivatives statistics at end December 2021.

[2]The statement is the result of internal computations undertaken by the author on confidential EMIR data and are *limited* to the jurisdictions overviewed by the ECB.

Markets Infrastructure Regulation (EMIR) which requires EU entities engaged in derivative transactions to report them to trade repositories (TRs) authorized by the European Securities Markets Authority (ESMA). To reduce counterparty credit risk, a clearing obligation through central clearing counterparties (CCPs) for standardized derivative products and stricter margining practices were introduced. Under the current EMIR technical standards precise clearing thresholds are set by class of OTC derivative contracts, which determine whether Financial counterparties (FC) and Non-Financial counterparties (NFC) are subject to clearing obligations through CCPs. Whenever a derivative trade is not centrally cleared, risk mitigation techniques must take place and the regulation requires counterparties to exchange variation margins (VM) and initial margins (IM).

Both IM and VM are used as collateralization instruments and will be used in this paper to uncover the network structure of non-centrally cleared derivative exposures. The IM is posted at the beginning to enter a derivative contract and it is intended to cover potential losses arising in the period between the defaulter's last variation margin payment and the point in time at which the surviving party is able to hedge or replace the trade. The higher the IM posted the higher the wealth at stake in that bilateral transaction. The amount of IM can be recalibrated over time especially in period of high market volatility (i.e. re-coverage of portfolios' riskiness). The VM is used to compensate daily fluctuations in the market value of the derivative contract instead. Given a certain variation in the price of the underlying instrument, the counterparty negatively affected by the price variation is required to pay a certain amount of money accordingly. Then, the IM network will reflect the riskiness in terms of potential future losses of the derivative exposures while the VM network constitutes, for a given time span, the liquidity flows of money between the involved institutions.

Two main findings will be highlighted in the paper. First, the channels containing the highest exposures, and identified through the proposed filtering tool, involve mainly institutions belonging to jurisdictions outside the euro area (EA). Second, both initial and variation margin networks display anomalous behaviors in the power-law parameter associated respectively to both the degree and in/out-strength distributions, signaling the presence of extreme positions and liquidity outflows during turmoil periods to be brought to the attention of policy makers and supervisory authorities.

The article is organized as follows: In section 2 I briefly review the literature on empirical and network studies that contributed to this strand of research on financial derivatives; in section 3

I describe the dataset and the way I cleaned the data to build it; in section 4 I analyze both the IM and VM networks, emphasizing their structural properties and subsequent potential implications; conclusion and discussions are finally provided in section 5.

2 Literature Review

The literature on the network structure of derivative markets is particularly small due to lack of access to confidential and regulatory data. On the empirical side, given the 2008 financial crisis and subsequent sovereign debt crises, the literature started to implement network approaches to monitor and assess systemic risk arising from CDS markets and potential contagion channels through highly interconnected institutions (Markose et al., 2012; Brunnermeier et al., 2013; Cetina et al., 2018). All these studies confirmed the importance of monitoring CDS exposures given their level of concentration in the market and the presence of potential 'super-spreaders' of contagion, with some banks having exposures larger than their equity as shown by Clerc et al. (2014). Duffie et al. (2015) also used bilateral CDS positions to estimate the impact of clearing and margining practices on collateral demand A detailed analysis on the network structure of the CDS markets can be found also in Peltonen et al. (2014), where the economic determinants of the network and its emerging properties were econometrically investigated using a relatively large sample of 642 entities transacting in the CDS market.

Another strand of literature focused instead on CCPs stability, investigating the riskiness of their clearing members positions and the effectiveness and structure of the client-clearing intermediation process. Despite the general agreement on the crucial role played by CCPs in reducing counterparty credit risk in derivative transactions, Duffie and Zhu (2011) provided an interesting assessment for the role of CCPs and critically analyzed the impact of central clearing on counterparty risk. Wide descriptive analyses of the client-clearing network and the structural properties of derivative markets were especially provided for the euro area (EA) (Abad et al., 2016; Rosati and Vacirca, 2019; Kahros et al., 2021), with a focus on the description of fundamental network metrics and technical explanations on CCPs and clearing member activities. Concentrating risks in CCPs and their implications for network stability in OTC derivative markets have been widely investigated also by Heath et al. (2016), where data on margins were simulated, given the lack of access to regulatory data, using aggregate balance sheet data and

historical time series prices to calibrate the simulations[3].

The network structure of OTC derivative markets in UK have been examined also by Bardoscia et al. (2019) who highlighted the usefulness of network centrality measures as proxies for the vulnerability of clearing members, and the potential liquidity risk they may face because of the directionality of their portfolios. The liquidity risk faced by clearing members under different stress scenario has been investigated also recently by Bardoscia et al. (2021) who used trade repository data for a sample of 103 clearing members.

With respect to the current literature, this contribution is manifold. First, I shed lights on that part of the derivative market that is not subject to central clearing and which has not been sufficiently covered in the literature. I thus provide insights on the implications of the detected network structures from a financial stability point of view. Second, differently from previous studies, I include in the sample all the transacting entities reporting to the EMIR infrastructure. Moreover, to have a complete view about the overall exposure for each reporting institution, I collect initial and variation margin data across all the different kind of derivative instruments (mainly Swaps, Futures/Forward and Options) and underlying asset classes (mainly Interest Rates, Credit, Equities and Commodities). This leads to a very large network. I thus propose the adoption of a filtering tool to extract relevant information from the initial margin network, selecting a subset of exposures that might generate large losses for counterparties. Finally, I contribute to the literature by providing a reference table containing estimates and non-confidential topological information on the variation margin network. This might enable researchers to simulate derivative networks in a more realistic way, to study liquidity risk and contagion, even with no access to regulatory data.

3 Data description

EMIR requires counterparties to report their derivative transactions to the TRs. All derivative transactions, both centrally cleared and bilateral contracts, should be reported independently of whether traded on exchange trade derivatives (ETD) markets or on OTC markets. The regulation applies to financial intermediaries as well as to non-financial companies with positions

[3]Precisely, variation margins were simulated from a zero-mean Normal distribution. As it will be shown in the remainder of this paper, variation margins are all but normally distributed and zero-mean random variables unfortunately. As a consequence, liquidity stress stemming from derivative positions could be strongly underestimated under the Normality assumption.

above some thresholds defined by the regulation. It is a double reporting system, meaning the reporting obligation is on both counterparties. The TRs collect and maintain the records of the derivative contracts reported and make them available to the relevant authorities. The European Central Bank (ECB) is entitled to receive all the transactions in which at least one of the following situations hold true: i) At least one counterparty in the derivative transaction is resident in the euro area (i.e., a future contract between two counterparties being respectively in Germany and UK); ii) The reference entity is in the euro area (a CDS on a German bank, even if transacted between extra euro area institutions); iii) The reference obligation is the sovereign debt of a euro area country (i.e., a CDS on Italian debt).

The initial and variation margin used to reconstruct the two collateralization networks that I am going to analyze are reported by counterparties in EMIR at the portfolio level. Portfolios can include either different types of derivative instruments, different types of underlying in terms of asset class, or even both mixed asset classes and mixed contract types in the same portfolio. Thus, both initial and variation margin represent the riskiness of the overall portfolio position of the reporting counterparties. Each counterparty reports the amount of initial and variation margin posted and received on that portfolio position. It worth mentioning the reconstruction of the two networks become particularly challenging when the data reported by the two counterparties does not coincide, I thus refer the reader to the appendix for more technical details about the data collection process.

Since the focus is on the collateralization networks, the portfolios having no initial and variation margin posted have not been included in the sample independently from their notional size. The overall notional of the sampled non-centrally cleared transactions reporting initial and variation margin was 78 trillion of euro on 14^{th} February 2020. Figure 1 shows the percentage composition, in terms of both type of derivative instruments and underlying asset classes, of the notional of the portfolios for which initial and variation margins have been collected and computed to reconstruct the network.

4 Financial network analysis

I analyze two different networks of bilateral derivative transactions which are the initial margin and the variation margin networks. The network structures to be analyzed can be encoded in the adjacency matrices. I denote with $\boldsymbol{A} = (a_{ij})$ the binary adjacency matrix where $a_{ij} = 1$ if

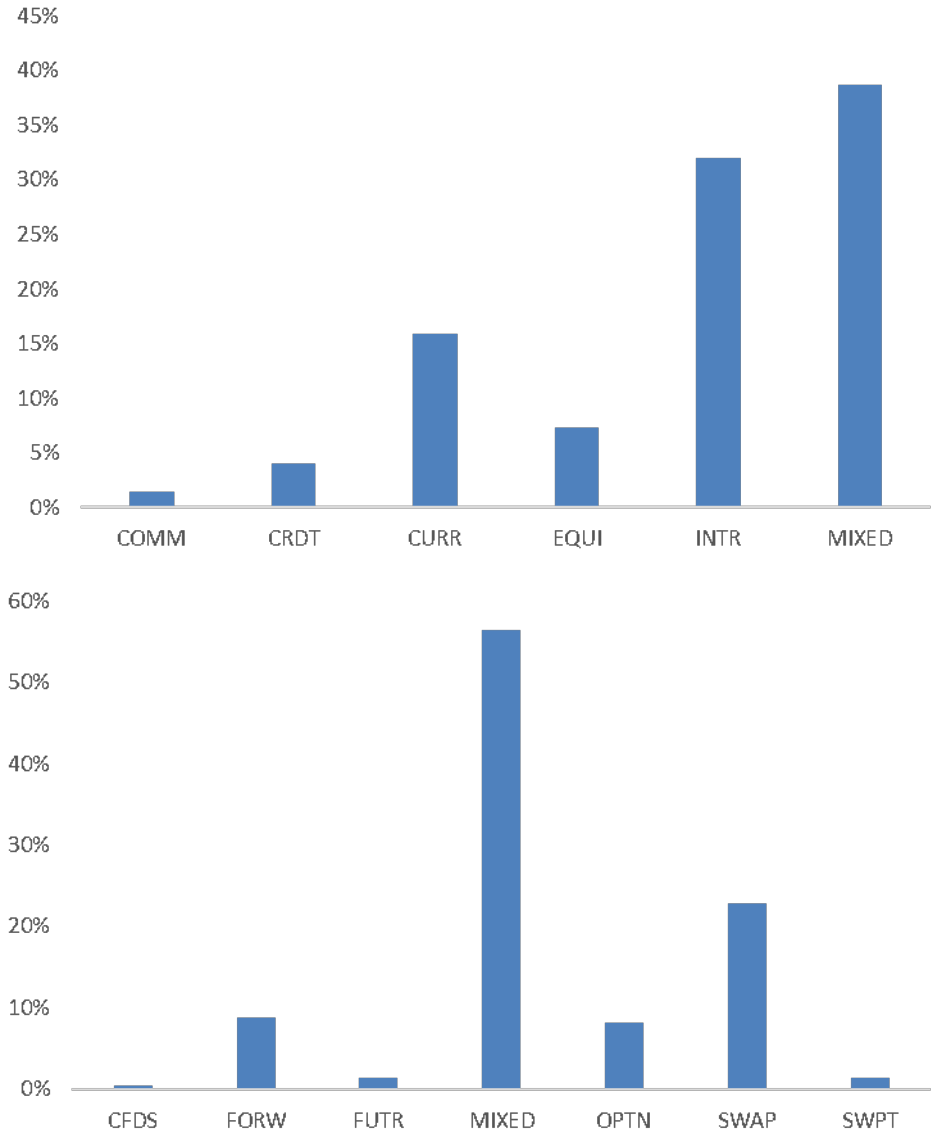

Figure 1: Almost 60 percent of the total notional size can be attributed to portfolios containing multiple derivative instruments. Almost 40 percent of the same notional can be attributed to portfolios containing multiple asset classes as underlying. The portfolios being mixed both in terms of derivative instruments and asset classes represent the 36 percent of the overall notional. For 'pure' portfolios, Swaps contracts (23 percent) are the mostly used, followed by Forward (9 percent) and Options (8 percent), with underlying being mostly interest rates (32 percent) and currencies (16 percent) followed in order by Equities (8 percent) and credit (4 percent).

there is a link between i and j (counterparties entered the contract and at least one of them posted either initial or variation margins) and 0 otherwise. with N being the set of nodes and E being the set of edges, the network is very large being $N = 36472$ and $E = 64978$ on 14^{th} February 2020 before the market turmoil caused by the Covid-19 pandemic. I consider also the weighted adjacency matrices $\boldsymbol{A}^w_{im} = (w^{im}_{ij})$ and $\boldsymbol{A}^w_{vm} = (w^{vm}_{ij})$ associated to the IM and VM networks respectively, where $w^{im}_{ij} = IM_i + IM_j$ is the amount of initial margin posted by the two counterparties (gross exposure) while $w^{vm}_{ij} = VM_{j\to i}$ is the flow of money from j to i. Thus, while the initial margin network is treated as an *undirected* network (both *weighted* and *binary*), the variation margin network will be analyzed as a *weighted directed* one since it represents money flowing between institutions. In the following, I provide a structural analysis of the two networks and potential policy implications.

4.1 The initial margin network

The network of financial derivative transactions is not fixed over time, the number of nodes and edges will depend on the period chosen for the analysis. However, as will be shown, there are general structural properties which are rather stable over time. I will particularly focus on the network structures on 14^{th} February 2020 and on 31^{st} March 2020, thus before and after the market turmoil caused by the Covid-19 pandemic.

I begin with local network measures, in particular Figure 1 shows the degree distribution in log-log scale before and at the end of the market turmoil. Despite the absence of central clearing through clearing members and CCPs, the network of bilateral derivative exposures is characterized by a statistical abundance of financial institutions with a very large number of interconnections (i.e. degree) k with respect to the average. This empirical feature has been observed for a wide variety of real-world networks finding its statistical description through scale-free degree distributions, meaning their functional form obeys a power law behavior $f(k) \sim k^{-\alpha}$. The power-law fit is obtained by implementing the Rank-1/2 approach (Gabaix and Ibragimov, 2011) and yields a rather 'anomalous' exponent $\alpha < 2$, meaning the degree distribution of the bilateral binary IM networks has no finite first and second moments. This topological feature is extremely relevant when assessing network robustness and vulnerability. Observing such a behavior for the derivative network implies robustness to random financial failures but fragility with respect to targeted attacks (Doyle et al., 2005; Gai and Kapadia, 2010; Tan et al., 2015), meaning that highly interconnected financial institutions must be appropriately hedged

to avoid cascade events. The derivative network is not the first real-world network showing that anomalous behavior of the tail-exponent (i.e. diverging mean and variance of the degree distribution), a similar estimate has been obtained also for the world-wide airport network (Barrat et al., 2004).

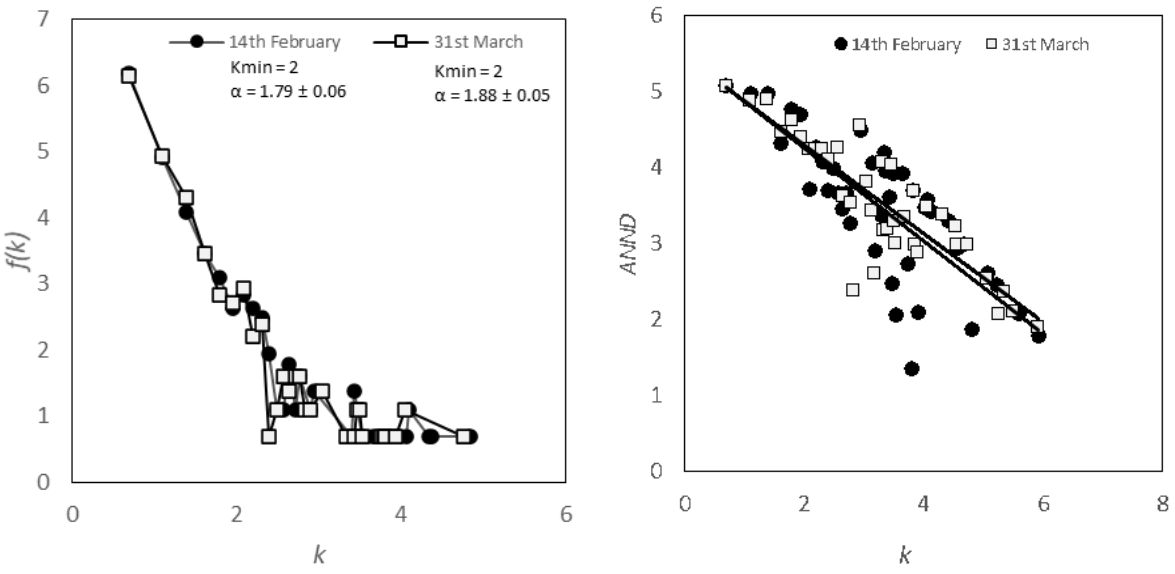

Figure 2: (left panel) Degree distributions of the IM network before and at the end of the Covid-19 market crash. The degree k corresponds to the number of counterparties each institution has posted initial margin to. The distributions are heavy-tailed, their functional forms have been approximated by the power-law behavior $f(k) \sim k^{-\alpha}$ with $\alpha = 1.79 \pm 0.06$ before the market crash and $\alpha = 1.8 \pm 0.05$. These values denote 'anomalous' behaviors since both the first and second moment diverge to infinite. (right panel) ANND-degree scatter plot. The negative trend indicate that high-degree entities tend to be interconnected with low degree entities (i.e. negative assortativity coefficient).

I then proceed by exploring possible (dis)assortative patterns in the bilateral IM networks. I start computing the average nearest neighbor degrees (ANND) and their correlation with the degrees. The negative trend displayed in the right panel of figure 2 implies the network to be disassortative, since financial institutions with many interconnections tend to be mostly connected to institutions poorly interconnected. To show the temporal stability of this disassortative behavior I calculate and plot over time the assortativity coefficient. Figure 3 displays a strongly disassortative and stable dynamics for the non-centrally cleared derivative network, comparing it with the assortativity of a network having the same number of nodes as the real one but randomly generated following Erdős et al. (1960). Disassortative patterns are not new in the empirics of financial networks, where interbank networks were mostly analyzed (Chinazzi

et al., 2013; Squartini et al., 2013; Bargigli et al., 2015; Fricke and Lux, 2015; Tonzer, 2015; Aldasoro and Alves, 2018) and core-periphery structures were detected and modeled to explain the emergence of disassortative mixing (Lux, 2015; Silva et al., 2016).

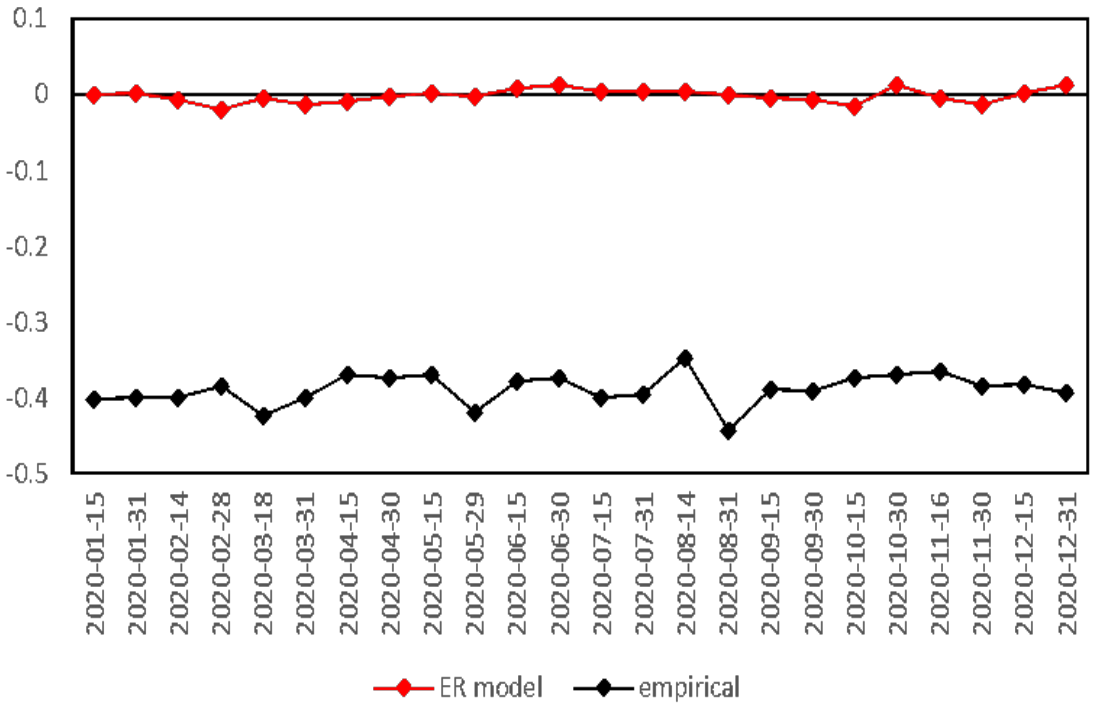

Figure 3: Assortativity coefficient over time for both the empirical and the ER random network with the same number of nodes. The non-centrally cleared derivative market is not random at all and display strong disassortative mixing patterns.

Network with a core-periphery are composed simply by two structures: the core and the periphery. Nodes in the periphery are linked only to core members, while core members are highly interconnected with each other forming cliques (complete subgraphs). Networks with a core-periphery display the so-called 'rich-club effect' and can be heuristically quantified through the rich-club coefficient. Differently from the interbank network, the presence of a core-periphery structure to explain the disassortative mixing does not seems to fit for the non-centrally cleared derivative network. While Silva et al. (2016) found the rich-club coefficient to range between 0.5 and 1 (depending on the threshold value for k) for the entities with several interconnections in the Brazilian interbank, I get relatively small rich-club coefficients, ranging between 0 and 0.25 for the most interconnected financial institutions as displayed in figure 4.

Given the disassortative patterns together with the presence of hubs in the network, and the

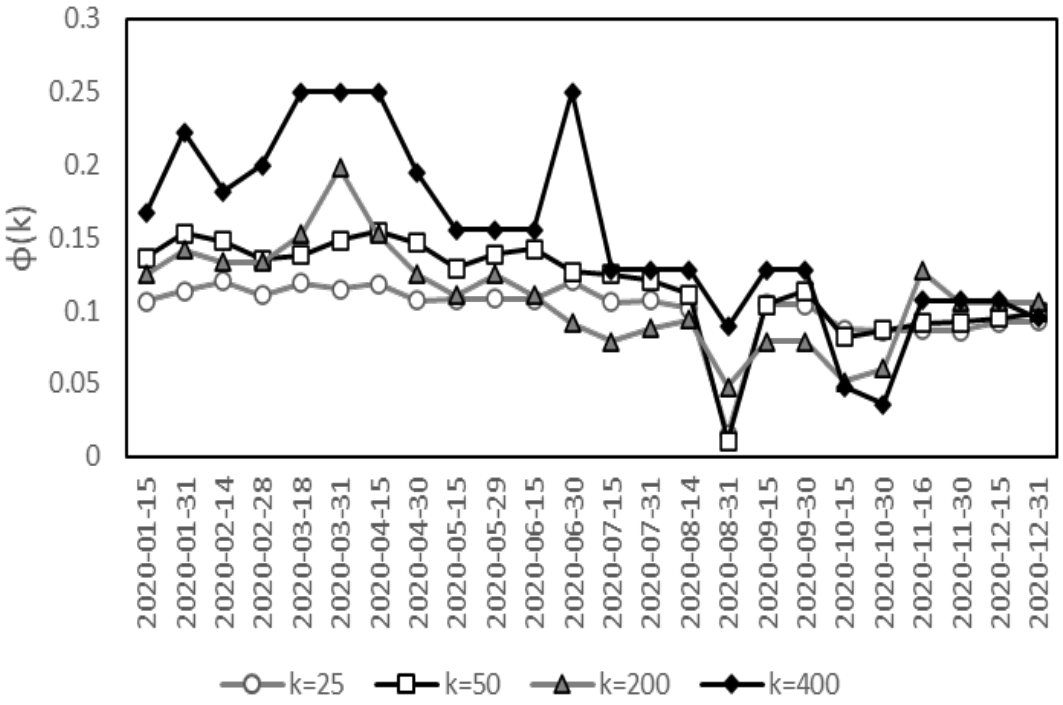

Figure 4: Rich-club coefficient over time. Even when considering FIs with large degrees, we do not find evidence for the presence of a core-periphery structure.

absence of a core-periphery structure, it seems reasonable to believe each financial institution acting as a hub to create its own community in a hierarchical network where all peripheral members (inside the community) connect only to community hubs. The procedure I am going to implement to partition our network in communities is the modularity maximization approach (Clauset et al., 2004; Newman, 2006). In the network science literature, the goal of modularity maximization is the uncovering of community of nodes whose internal interactions are both stronger compared to the inter-community ones and maximally unexplained by a null model taken as benchmark. To check the robustness of the detected communities (i.e. ensuring the partitioning does not heavily depend on the methodological approach chosen) I follow also the Infomap approach of Rosvall and Bergstrom (2008) and compare the results[4]. I then check the temporal stability of the detected partitions by computing an information-theoretic measure known as *variation of information* (VI) which can be used to quantify the difference between two partitions (Meilă, 2007). Given two partitions of the nodes at two different points in time,

[4]The codes are publicly available in the igraph R package.

γ^t and $\gamma^{t+\delta t}$, the VI is defined as

$$\begin{aligned} VI(\gamma^t, \gamma^{t+\delta t}) &= [H(\gamma^t) - I(\gamma^t, \gamma^{t+\delta t})] + [H(\gamma^{t+\delta t}) - I(\gamma^t, \gamma^{t+\delta t})] \\ &= H(\gamma^t|\gamma^{t+\delta t}) + H(\gamma^{t+\delta t}|\gamma^t) \end{aligned} \tag{1}$$

where $I(\gamma^t, \gamma^{t+\delta t})$ is the *mutual information* between the two partitions while $H(\gamma^t)$ and $H(\gamma^{t+\delta t})$ are their *entropies*. These terms can be rearranged in the two conditional entropies which measure respectively the amount of information lost about γ^t and the one that must be gained about $\gamma^{t+\delta t}$ when moving from γ^t to $\gamma^{t+\delta t}$. The VI measure possesses some desirable properties: it satisfies all the metric axioms (i.e. it is a real distance), is bounded from above by $\ln N$ to control for the magnitude of the variation among clusters, making possible to compare clustering across datasets and across algorithms as well[5]. Both the modularity maximization and the Infomap approach reveal a rather dynamic structure with around a 60 percent change in community structure month by month, meaning many nodes change each month the community to which they belong. This behavior is confirmed across different community detection methodologies, since both the modularity and the Infomap approach yielded very consistent results in terms of stability over time as shown in figure 5. In the right panel of the same figure I also plot the average degree $|k|$ computed inside a given community versus the size of the latter comparing again the results across the two different community detection approaches. Results are again quite consistent: the two approaches manage to identify almost perfectly the smaller communities and the largest one, with the only difference being that the modularity approach cluster together a group of nodes in one large community (the second one in terms of size) while the Infomap approach split the same large group in two distinct communities. Apart from this discrepancy in the size and associated degrees of two communities, the rest of the clusters closely overlap suggesting the presence of dynamic community structures over time.

I look then at the average path length (APL). Many real-world networks exhibit the so-called 'small-world' property. Being 'small-world' means in technical terms to observe a network diameter $D \sim \ln N$, meaning the shortest distance between the two most distant nodes increase very slowly with the number of nodes. However, the derivative networks in the non-centrally cleared space in this sense is very small, being the APL $\sim \ln(\ln N)$ and pointing in favor of an 'ultra-small world' phenomena (Cohen and Havlin, 2003) as typically observed in randomly

[5]For more details I refer the interested readers to Meilă (2007) and to Appendix A.

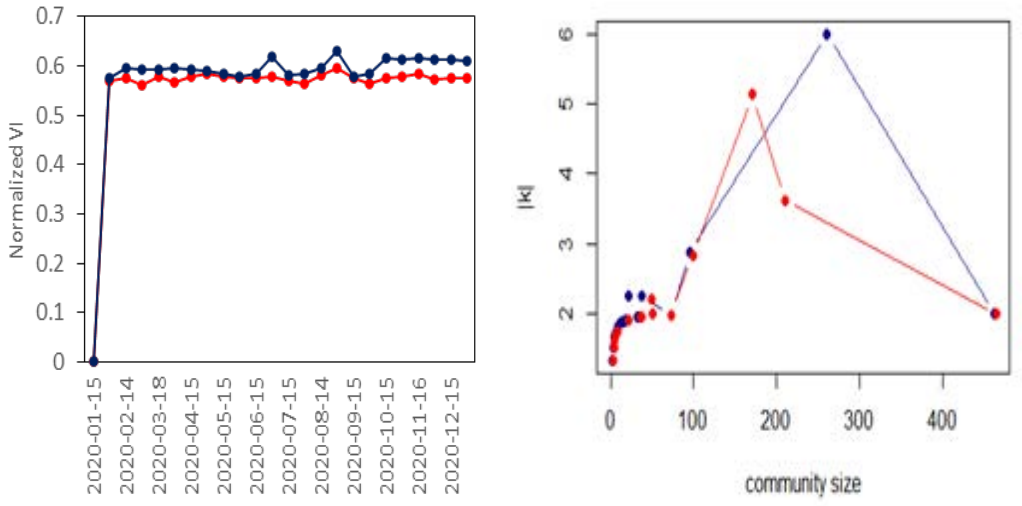

Figure 5: (left panel) Community structure stability through Variation of Information (normalized) over time. Comparison made for communities detected using both the modularity maximization (Louvain algorithm implementation, blue color) and the Infomap approach (red color). (right panel) Average degree inside a given community versus community size (i.e., number of entities inside that community).

generated scale free networks (Barabási and Albert, 1999). In figure 6 the empirical APL of the derivative network is computed and plotted over time. To give an idea of the magnitude of the ultrasmall world effect the empirical APL is compared with the one we would observe, keeping the same number of nodes at each point in time, in a random network generated following (Erdős et al., 1960).

The presence of an ultra-small derivative market even without central clearing is particularly relevant for policy makers and could act as a double-edged sword: Adverse shocks can propagate in the network affecting many institutions very quickly, at the same time being the network ultra-small is much faster to identify many critical channels of contagion. The first typical and smart approach is the surveillance of highly interconnected and large institutions. Still, understanding which channels should be monitored starting from these nodes is not easy in such large and complex networks. In what follows, the adoption of spanning trees will be proposed as filtering tools to select the channels linking all the institutions in the fastest way and with the maximum level of exposure. The tool might be complementary to other well-established supervision approaches adopted in the regulation and by policy makers.

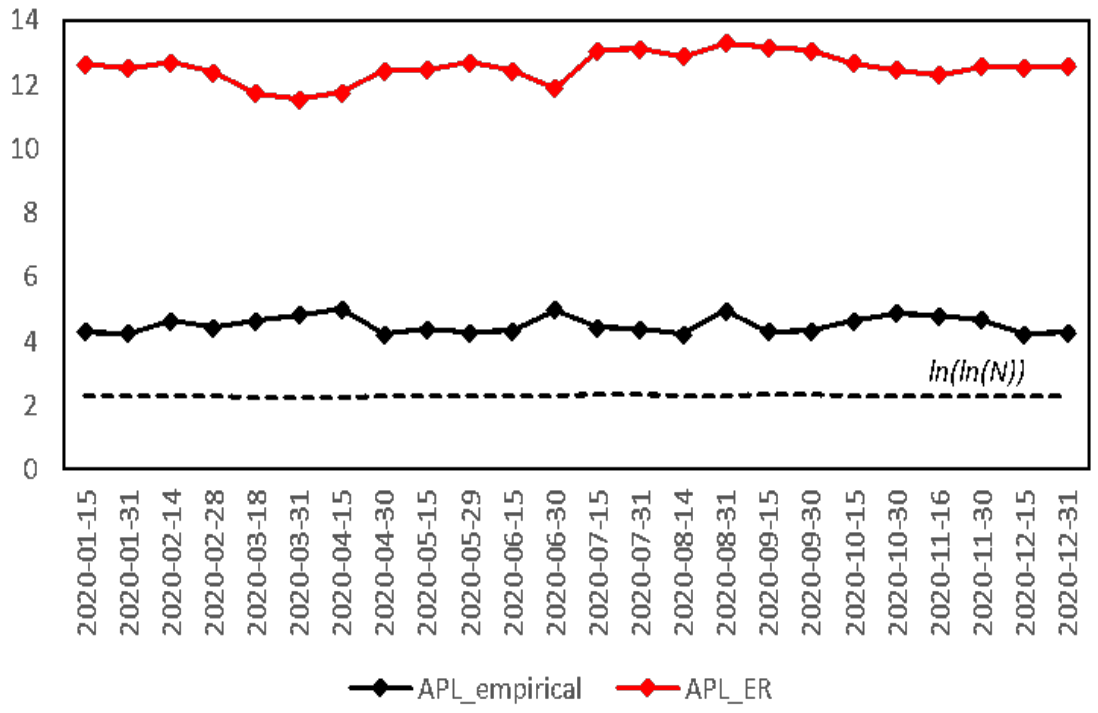

Figure 6: Average Path Length over time for both the empirical and the ER random network with the same number of nodes. Random networks are capable to reproduce the so called 'small world' phenomena. The derivative network displays a very short APL which closely track even the logarithm of the logarithm of N, pointing in favor of an 'ultra-small' world.

4.1.1 Identifying the maximum exposure channels: The Maximum Spanning Tree approach

Since the seminal work of Mantegna (1999) on the hierarchical structures of financial markets, Minimum Spanning Trees (MST) have been mainly used in the literature to filter out relevant information from stock markets for both asset allocation purposes (Onnela et al., 2003; Tumminello et al., 2010; Peralta and Zareei, 2016; Raffinot, 2017) and the structural analysis of financial market dynamics during the Covid-19 global pandemic (Zhang et al., 2020). Given the complexity of derivative transactions and their relevance from a financial stability perspective, I propose in this work the adoption of Spanning Trees to filter out a subgraph containing the highest derivative exposures in the non-centrally cleared derivative network.

Definition 1 (Spanning Tree). *Given a graph $G = (N, E)$, with N being the set of nodes and E being the set of edges, a Spanning Tree is a connected acyclic undirected subgraph of G connecting all the nodes in G.*

Definition 2 (Maximum Spanning Tree). *Given a weighted connected graph $G = (N, E, W)$, with N being the set of nodes, E being the set of edges, and W being the set of weights, a Maximum Spanning Tree (Max-ST) is a spanning tree T of G maximizing $\sum_{e \in T} W(e)$.*

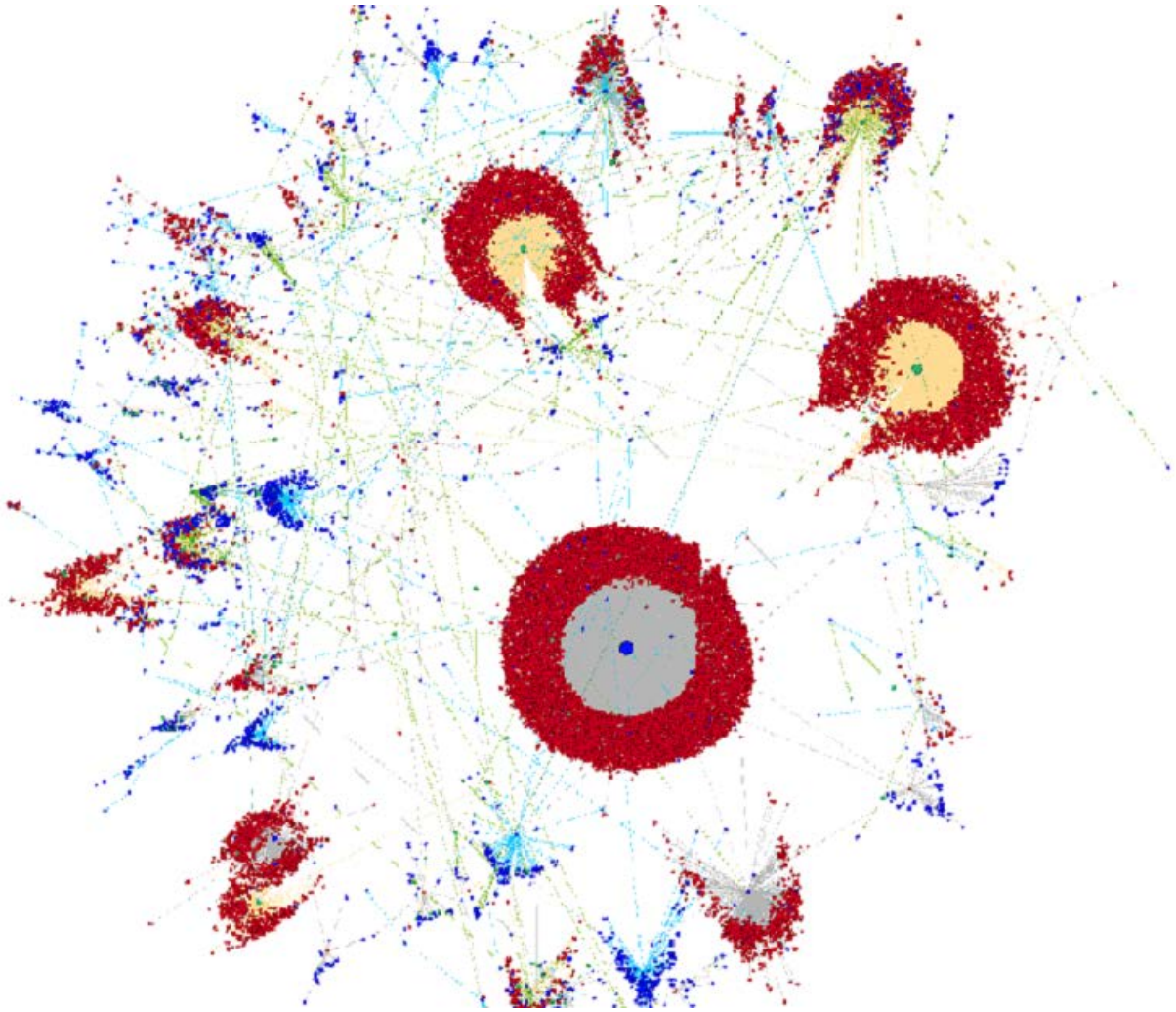

Figure 7: Graphical representation of the Max-ST of the initial margin network. Nodes in blue represent companies in the EA, green represents European Union (EU) but not EA, red represent companies outside the EU. The edges in gray link EA with extra-EU nodes, yellow edges connect EU (but not EA) to extra-EU nodes, green edges connect EU to EU nodes while light blue connect EA to EA nodes.

The approach is conceptually identical to the MST with the crucial difference that I am going to maximize the weight of the path which goes through all the financial institutions, leading then to the Maximum Spanning Tree (Max-ST). Being the general weight of an edge $w_{ij}^{im} = IM_i + IM_j$, the Max-ST then contains a subgraph characterized by N nodes and N-1 edges for which the

amount of initial margins is maximized. This is crucial from a policy perspective since the biggest exposures in terms of potential losses are those to be closely tracked and supervised. This filtering procedure can be very useful from a macroprudential perspective. When comes to assessing financial stability is fundamental to both focus on sizeable exposures and act in a timely manner to avoid contagion in the financial system. In complex networks characterized by large amount of transactions as in the financial derivative markets, it is very hard to keep the focus on the entire system under control without losing crucial information on some of its entities. To this end, the Max-ST network possesses two interesting properties. First, all the financial institutions are connected in the tree with the minimum amount of links needed, meaning that is always possible to find a path on the tree to reach one financial institution starting from another one since the N-1 edges connects all the N entities. This allow the supervisors to focus on a small subset of transactions instead of tracking all of them and without removing any financial institution from the sample. Second, the path directly connecting (i.e., no cycles) two generic institutions on the tree has the maximum possible weight, meaning that in case of a default event triggering contagion through multiple steps, the potential loss for the system would be the maximum one.

The graphical representation of the Max-ST is provided in figure 7, while in figure 8 the degree distribution is shown together with additional information on the jurisdictions involved in the transactions. As expected, same fat-tail behavior is observed as for the entire IM network. More interestingly, around 90 percent of the exposures on the maximum spanning tree represent transactions with counterparties outside the EA. Being the greatest exposures across jurisdictions, strict cooperation among authorities and policy makers is highly needed to implement effective supervision practices for global financial stability purposes. I now move to the analysis of the directed variation margin network, thus focusing on the liquidity flows faced by the nodes in the network during the Covid-19 market turmoil.

4.2 The variation margin network

Variation margins are exchanged in cash at least daily to reflect mark-to-market changes on counterparties' outstanding position caused by price changes on the underlying of the derivative instrument. They thus represent flows of money moving from one counterparty to another and can be at the origin of liquidity stress for counterparties. As for the initial margin network, I

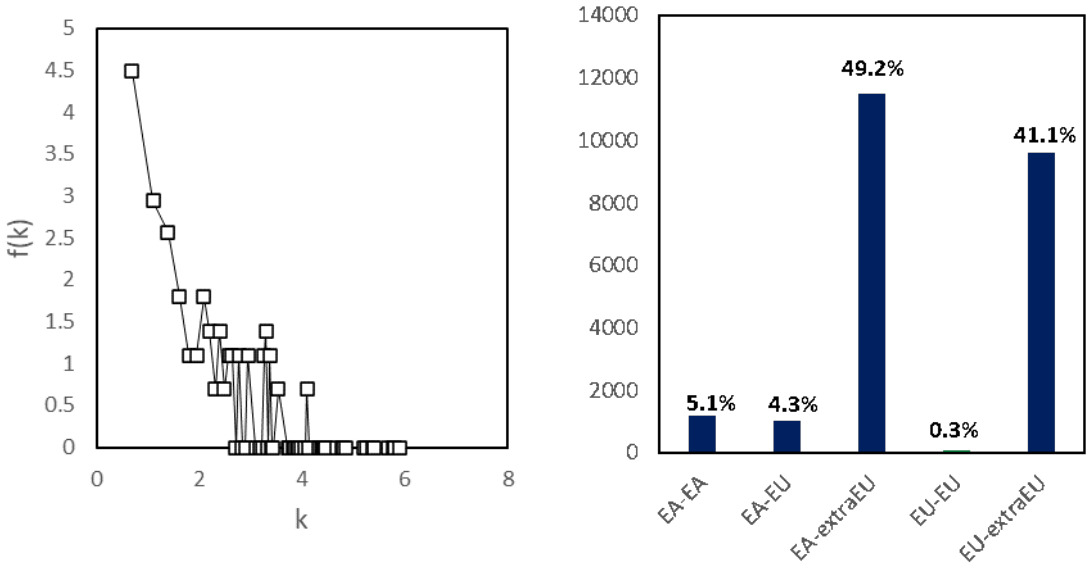

Figure 8: Degree frequency of the Maximum Spanning Tree on a log-log scale (left) and jurisdictions in which the largest exposure take place. Around 90% of the exposures laying on the Max-ST represent cross-border transactions between EA/EU and extra EU counterparties.

collect variation margin flows over the period 14^{th} February-31^{st} March 2020 in order to include the market crash caused by the beginning of the Covid-19 pandemic. Recalling the weighted adjacency matrix to be $A^w_{vm} = (w^{vm}_{ij})$ with $w^{vm}_{ij} = VM_{j\to i}$ the flows of money from j to i, I start focusing on the out-strength and in-strength distributions in order to capture the liquidity outflows and inflows faced by institution during the market turmoil. I also compute the overall strength for each node so to identify losers and gainers, over the period of interest (i.e., overall positive strength simply means the inflows were larger than the outflows and vice versa), showing their distributions as well. The out/in-strength measure for a generic node i then read simply as

$$S^{Out}_i = \sum_j w^{vm}_{ji} \tag{2}$$

$$S^{In}_i = \sum_j w^{vm}_{ij} \tag{3}$$

while the overall strength (net inflows/outflows) by consequence read as $S_i = S^{In}_i - S^{Out}_i$. All these strength measures tell us how the wealth at stake via bilateral derivative transactions has been distributed among transacting entities during the Covid-19 market turmoil.

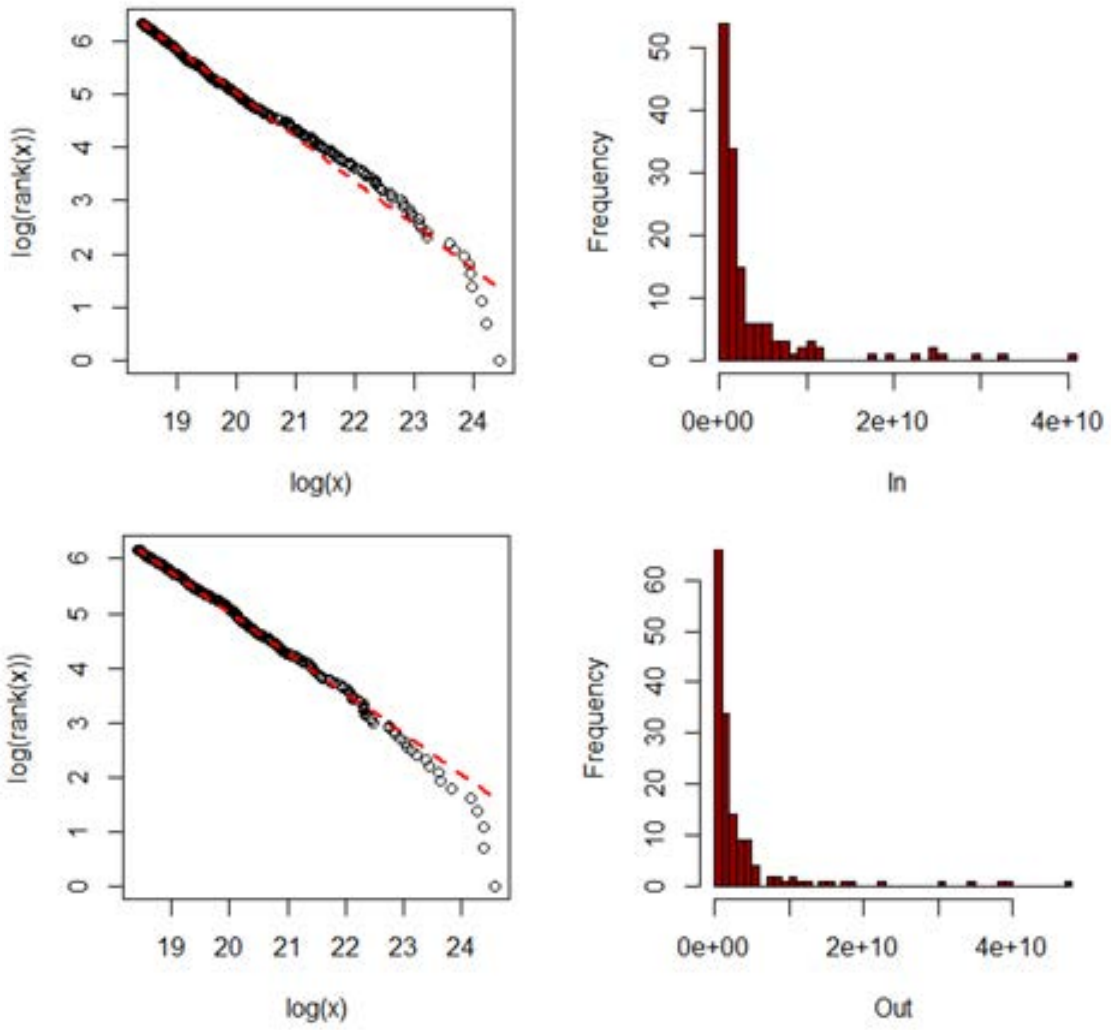

Figure 9: In-strength and out-strength distributions on a log-log scale (left panel) and empirical frequency distributions (right panel).

Variation margins can be exchanged even when no initial margin is required to enter the derivative contracts, which typically happens for very small exposures among counterparties. This makes the variation margin network very dense and full of very small transactions almost negligible from a financial stability perspective and which would spike the distribution over zero. I thus reconstructed the network setting a relatively low edge threshold $\tau = 10 million$, meaning we remove all those 'small' positions that generated less than 10 million of cumulative inflows/outflows over the analyzed period of the present analysis. Figure 9 then displays the in-strength and out-strength distributions respectively from which it is possible to appreciate the fat-tail behavior typically observed in many real-world networks. These distributions conceptu-

ally are, as matter of fact, wealth distributions where we can appreciate that a small fraction of entities accounts for a very large fraction of the overall money flows in the system. I then model the distributions as Pareto type I distributions which can be written as

$$F(x) = 1 - \left(\frac{x_{min}}{x}\right)^{\alpha}, \qquad x_{min} > 0, \alpha > 0 \tag{4}$$

The maximum likelihood estimator (MLE) of x_{min} is straightforward, since it is the minimum of the sample and given our network structure it coincides with the previously mentioned threshold τ=10 million. Given the known $x_{min} = \tau$, we estimate the MLE $\hat{\alpha}$ of α. Note that the MLE of α is biased but consistent. Moreover, given the size of our network the bias is entirely negligible and does not affect our results. The estimates yielded $\hat{\alpha}$=0.6369 and $\hat{\alpha}$=0.6563 for the in-strength and out-strength distributions respectively. The estimates imply both the first and second moments of the distributions to diverge to infinite asymptotically with the number of entities transacting in derivative markets (we refer the readers to the Appendix for more details on the consistency of the estimates and diverging moments). This bring tremendously important policy implications. Diverging moments for the out-strength distribution imply the presence of extreme outflows worsening liquidity stress during market crashes and thus calling for central banks' interventions. I then look at the overall strength distributions, splitting the sample between those entities which lost ad those which earned money over the period of interest. For these net-wealth distributions estimates yielded $\hat{\alpha}$=0.6697 and $\hat{\alpha}$=0.7036 for the net inflows and net outflows respectively, signaling extreme earnings and losses behavior in non-centrally cleared derivative markets during the Covid-19 market crash.

It is worth noticing the results might depend on the threshold τ=10 million used to focus on a subset of significant transactions in the market. It is interesting to check the sensitivity of the results with respect to τ. These estimates on real data could act as a reference for future network analyses on derivative markets, since bilateral transactions data are not publicly available and have to be simulated starting from aggregate data. I then reconstruct the network using different thresholds and I estimate again α for each threshold adopted. The results in table 1 show how both the size of the network (in terms of edges and nodes) and the parameter's estimates change when different threshold values are used. The overall message of the estimates is rather clear: Both first and second moments for the distributions are diverging to infinite, the only exception is when I focus on a very small network of 144 transacting entities (i.e. τ=500 million) with

finite first moment but still a diverging variance for the net-inflows/outflows.

$\hat{\boldsymbol{\alpha}}$	In-strength (inflows)	Out-strength (outflows)	Net inflows	Net outflows
$\tau = 1$ million $N = 5652$ $E = 26276$	0.4322	0.4596	0.4456	0.4841
$\tau = 10$ million $N = 2351$ $E = 8782$	0.6369	0.6563	0.6697	0.7036
$\tau = 100$ million $N = 561$ $E = 1349$	0.8291	0.7378	0.9722	0.8154
$\tau = 500$ million $N = 144$ $E = 167$	0.8341	0.7674	1.122	1.092

Table 1: Estimates table for the Pareto type I's parameter α for different network structures induced by the threshold chosen. Always diverging second moment, almost always non-finite mean.

It is worth mentioning that institutions involved in non-centrally cleared transactions might be transacting at the same time in the centrally cleared space as well. Then, one could argue that extreme counterparties' positioning and liquidity outflows in the non-centrally cleared space might be there to simply hedge the exposures in the centrally cleared space and vice versa. In this case, those bilateral outflows would not cause liquidity stress since they would be netted by the inflows stemming from other exposures with different positioning strategies in the centrally cleared space. For this reason, for each of the sampled institutions acting in the non-centrally cleared space, I control for the presence of inflows stemming from the centrally space. In practice, I compute the following quantity

$$S_i^{hedged} = Out_i^{ncc} - In_i^{cc}$$

to check to which extent the outflows previously shown were counterbalanced by inflows in the cleared space. Figure 10 displays the distribution of S^{hedged} on a log-log scale, together with a scatter plot showing for each outflows in the non-centrally cleared space the associated inflows in the centrally cleared one. As expected, hedging activity is in place to some extent and outflows and inflows in the two spaces tend to be positively correlated at the counterparty level. For some counterparties, inflows completely offset outflows. Still, hedging between the two spaces

is only partial and many counterparties experience large net-outflows. Two main facts can be graphically appreciated in figure 10 indeed. First, inflows from centrally cleared exposures cover outflows in the non-centrally cleared space only partially. Second, even when offsetting outflows with inflows across the two spaces, extreme outflows appearing in the right tail of the distribution are detected. Moreover, the ML estimate of the Pareto type-I coefficient yielded results implying diverging first and second moments as well.

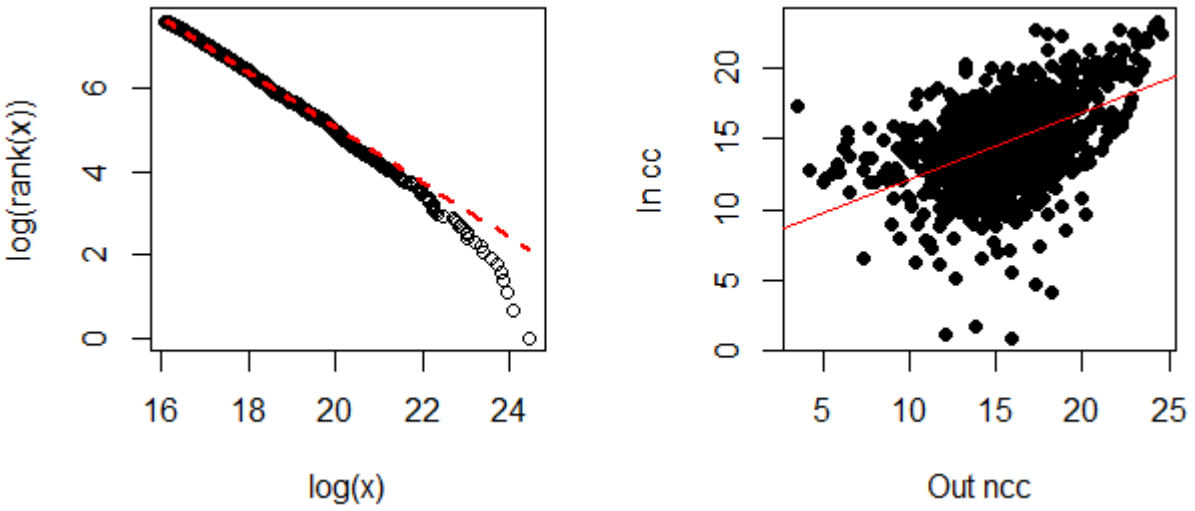

Figure 10: S_{hedged} distribution in log-log scale on the left hand side, with its two components Out_{ncc} and In_{cc} on a scatter plot on the right hand side.

For a complete and proper assessment of risk stemming from derivative exposures, it must be kept in mind that multiple hedging activities can be implemented by counterparties. One simple example would be the one in which a counterparty enters not only in derivative contracts (either cleared or not) with a long/short position but also in the underlying of the derivative but with opposite positioning. This would requires the access, for each counterparty, to each financial asset hold in their balance sheet and goes well beyond the scope and the possibilities of this work. Keeping in mind all of these warnings, this paper uncover for the first time a huge part of the non-centrally cleared derivative markets, shedding lights on its structure and capability to generate extreme positions and liquidity outflows which are not offset in the centrally cleared space for many counterparties. This lead us to the conclusions.

5 Concluding remarks

After the 2008 global financial crises, the regulators made tremendous efforts to make derivative markets transparent and safer through the requirement of strict risk mitigation techniques and the introduction of central clearing obligations to reduce counterparty credit risk. Despite the evident improvements, derivative instruments still embed substantial risks especially when used in opaque and non-prudential ways as shown by the default of Archegos in March 2021. Non-centrally cleared market constitute a substantial share of the overall derivative markets, but there is either little or no focus at all on these bilateral markets (possibly because of no access to such confidential data) in the current research literature which mainly focused on central clearing instead. This paper shed lights on the network structure of non-centrally cleared derivative markets, providing a detailed analysis of risks and liquidity dynamics under stressed periods. The non-centrally cleared network of derivative transactions is found to be scale-free even without the presence of central clearing counterparties, with anomalous exponents signaling the presence of extreme positions causing large liquidity outflows in stressed periods. Being the network 'ultra-small', acting in a timely in case of extreme losses is fundamental for policy makers to avoid contagion. Moreover, the highest exposures are across jurisdictions, calling for cooperation among different authorities.

Appendix A: Network metrics definitions

Average nearest neighbor degrees (ANND). Being A_i the i-th row of the adjacency matrix A the ANND for node i is computed as

$$ANND_i = \frac{\boldsymbol{A}_{(i)}\boldsymbol{A}\mathbf{1}}{\boldsymbol{A}_{(i)}\mathbf{1}}$$

and tell us what is, on average, the degree of the neighbors of node i.

Assortativity coefficient. It is the Pearson correlation coefficient of the degrees k_i, k_j at either ends of an edge e_{ij} (Newman, 2002), that is

$$\rho = \frac{1}{\sigma_f^2}\sum_{e_{ij}} k_i k_j (f_{(k_i k_j)} - f_{k_i} f_{k_j})$$

where f_{k_i} denotes the distribution of the remaining degree (i.e., total degree of a node on randomly chosen edge minus one), $f_{(k_i k_j)}$ denotes the joint distribution of the remaining degrees of the two nodes at either ends of the randomly chosen edge, σ_f^2 is the empirical variance of the degree distribution to normalize the coefficient.

Average path length (APL). It is the average of all the shortest paths connecting any possible pairs of nodes in the network. When the graph is binary, it becomes by construction the number of steps to be done on average along these shortest paths connecting any pairs of nodes. Thus, being $d_{(i,j)}$ the shortest distance between two generic nodes i and j, we have $APL = \sum_{i \neq j} d_{(i,j)}/N(N-1)$ where $N(N-1)$ is the total number of paths.

Modularity. The modularity $Q(\gamma)$ of a partition γ of the N nodes of a network is defined as

$$Q(\gamma) = \frac{1}{2m}\sum_{ij}(a_{ij} - E[a_{ij}])\delta(\gamma_i, \gamma_j)$$

where $2m = \sum_{ij} a_{ij}$ is the total edge weight in the network while $E(a_{ij})$ is the expected value of the entry of the adjacency matrix under a null model. Here the null model is the so-called configuration model (CM) which is used to randomize the network topology still preserving the empirical degree sequence. reads as $E(a_{ij}) = k_i k_j/2m$ and represents the probability for i and j to be randomly connected given their degree sequence and assuming a uniform probability

distribution over the edges. the Kronecker delta function $\delta(\gamma_i, \gamma_j)$ controls that only nodes belonging to the same community contribute to the increase in modularity when maximizing $Q(\gamma)$. The partition γ maximizing $Q(\gamma)$ is the one having community of nodes whose internal interactions are maximally stronger that the ones they would have under a null model taken as a benchmark.

Community tracking and the IV metric. Consider two partitions of the nodes into mutually disjoint subsets, obtained through any suitable clustering method at two different points in time, $\gamma^t = \{\gamma_1^t, \gamma_2^t, ..., \gamma_K^t\}$ and $\gamma^{t+\Delta t} = \{\gamma_1^{t+\Delta t}, \gamma_2^{t+\Delta t}, ..., \gamma_K^{t+\Delta t}\}$. I assume each node has the same probability of being picked, the probabilities of a generic node being respectively in the clusters γ_k^t and $\gamma_{k'}^{t+\Delta t}$ are $P(k) = n_k/N$ and $P(k') = n_{k'}/N$. I then follow Meilă (2007) quantifying the entity associated to the two partitions by computing their entropies

$$H(\gamma^t) = -\sum_{k=1}^{K} P(k) \ln P(k)$$

$$H(\gamma^t) = -\sum_{k'=1}^{K'} P(k') \ln P(k')$$

which is always non-negative and it is equal to zero when there is only one large cluster containing all the nodes (i.e., no uncertainty). I then quantify the information that one partitions has about the other by computing the *mutual information* as follows

$$I(\gamma^t, \gamma^{t+\Delta t}) = \sum_{k=1}^{K} \sum_{k'=1}^{K'} P(k, k') \ln \frac{P(k, k')}{P(k)P(k')}.$$

The VI metric computed as

$$\begin{aligned} VI(\gamma^t, \gamma^{t+\delta t}) &= [H(\gamma^t) - I(\gamma^t, \gamma^{t+\delta t})] + [H(\gamma^{t+\delta t}) - I(\gamma^t, \gamma^{t+\delta t})] \\ &= H(\gamma^t|\gamma^{t+\delta t}) + H(\gamma^{t+\delta t}|\gamma^t) \end{aligned}$$

represent the overall amount of information that we lose plus the we must gain when we move from clustering γ^t to clustering $\gamma^{t+\Delta t}$. The higher the metric the lower the stability of the detected communities. The VI can be normalized by using its upper bound which is the $\ln N$, so $NVI = VI/\ln N$.

Appendix B: Pareto-type I estimation details

I estimate the coefficient α of $F(x) = 1 - (x_{min}/x)^{\alpha}$ by maximum likelihood. Assuming $X_1, ..., X_N$ to be independent and identically Pareto distributed random variables, the MLE of α can be easily derived and is equal to

$$\hat{\alpha} = N / \sum_{i=1}^{N} \ln \frac{X_i}{x_{min}}.$$

When $\alpha < 1$ as in the VM networks analyzed, both firsts and second moments of outflows and inflows diverge to infinite since

$$E(X) = \int_{x_{min}}^{\infty} x \frac{\alpha (x_{min})^{\alpha}}{x^{\alpha+1}} = \alpha (x_{min})^{\alpha} \int_{x_{min}}^{\infty} 1/x_{\alpha} = \alpha (x_{min})^{\alpha} \left[\frac{x^{1-\alpha}}{1-\alpha} \right]_{x_{min}}^{\infty} = \infty$$

which signals the presence of extreme liquidity outflows and inflows on derivative positions in non-centrally cleared markets. Analogous computations follows for the second moment as well. As shown in Rytgaard (1990) the MLE of α is biased but consistent, since $E(\hat{\alpha}) = \alpha N/(N-1)$. Going back to Table 1 which contains the reference estimates for the different VM networks associated to different thresholds, N is sufficiently large and I can rely on the consistency of the estimates.

Appendix C: Details on data collection and cleaning

Dealing with misreporting. Each trade must be reported in EMIR by both counterparties, however both initial and variation margins are not reported at the trade level but at the portfolio level. Initial and variation margins for the counterparties should be the result of the riskiness of their overall exposures and would not make sense to compute them on a single trade basis indeed. In practice, what appears in EMIR is the following (pseudo EMIR table),

Trade Id	Portfolio code	Reporting cpty	Other cpty	Contract type	Asset class	Notional	IM(VM) posted	IM(VM) received
01	AB	A	B	Options	Equities	1000	50	10
02	AB	A	B	Futures	Equities	2000	50	10

where margins are, in principle, the same for different Trade id whenever they belong to the same portfolio (the example shows the typical case in which a portfolio contains different derivative instruments). We then have to sample margin only once for each portfolio. However, two errors

might appear in the data posing serious challenges for network reconstruction:

1 *Misreporting of the margins across different Trade id.* What if the margin posted for Trade id 02 is not equal to 50? It can happen to observe different but very close numbers for the margins reported in EMIR. The table below provide a concrete example. In this situation, I always take the maximum amount of margin reported by the counterparty.

Trade Id	**Portfolio code**	**Reporting cpty**	**Other cpty**	**Contract type**	**Asset class**	**Notional**	**IM(VM) posted**	**IM(VM) received**
01	AB	A	B	Options	Equities	1000	**50**	10
02	AB	A	B	Futures	Equities	2000	49	**11**

2 *Counterparties report different data.* In the tables above, for simplicity, only A has been illustrated as the reporting counterparty. However, as already mentioned, EMIR is a double-reporting based system. What could happen, as shown in the table below, is the situation in which the amount of margin posted by A to B (according to A) is different from the amount of margin that B received from A (according to B).

Portfolio code	**Reporting cpty**	**Other cpty**	**Notional**	**IM(VM) posted**	**IM(VM) received**
AB	A	B	3000	**50**	10
AB	B	A	3000	**15**	40

Whenever this situation happens, I always choose the posted as the default option: What B has received from A will not be what B reported in the received field but what A reported in the posted field, and vice versa. Then, the final table with consistent data will be the one below.

Portfolio code	**Reporting cpty**	**Other cpty**	**Notional**	**IM(VM) posted**	**IM(VM) received**
AB	A	B	3000	50	15
AB	B	A	3000	15	50

For the initial margin network, the link between A and B would be then an undirected link having weight $50+15=65$. For the variation margin network, since variation margins are also reported at the stock level, I compute for each pair of nodes the net amount of variation margin (VM posted – VM received) and then I take the first difference over time of this quantity (given the period of interest chosen, which was the Covid-19 turmoil here)

to get the money flowing from one counterparty to the other.

Identifying non-centrally cleared trades. In EMIR different variables are available to allow us to identify, through internal coding procedure, whether:

1 A clearing obligation holds for that transaction (TRUE/FALSE variable)

2 One of the two counterparties is either a CCP (central counterparty) or a clearing member belonging to a CCP

3 Clearing is in place for the trade (Yes/No variable)

These information are sufficient to understand whether a portfolio was subject to central clearing or not (or partially, meaning only some trades composing the portfolio have been cleared). Moreover, it worth mentioning that a clearing member is not always acting necessarily on behalf of its clients (clearing the trades for them) and might engage in bilateral transactions with other institutions. All the data used in this analysis are such that: i) Only portfolios that are 100 percent non-centrally cleared have been sampled; ii) No CCPs appear either as reporting or other counterparty; iii) when a clearing member appears either as reporting or other counterparty it is because the portfolio associated to those transactions has not been cleared, meaning the clearing member is reporting a bilateral trade and not a clearing process on behalf of its clients.

References

Abad, J., I. Aldasoro, C. Aymanns, M. D'Errico, L. F. Rousová, P. Hoffmann, S. Langfield, M. Neychev, and T. Roukny (2016). Shedding light on dark markets: First insights from the new eu-wide otc derivatives dataset. *ESRB: Occasional Paper Series* (2016/11).

Aldasoro, I. and I. Alves (2018). Multiplex interbank networks and systemic importance: An application to european data. *Journal of Financial Stability 35*, 17–37.

Barabási, A.-L. and R. Albert (1999). Emergence of scaling in random networks. *science 286*(5439), 509–512.

Bardoscia, M., G. Bianconi, and G. Ferrara (2019). Multiplex network analysis of the uk over-the-counter derivatives market. *International Journal of Finance & Economics 24*(4), 1520–1544.

Bardoscia, M., G. Ferrara, N. Vause, and M. Yoganayagam (2021). Simulating liquidity stress in the derivatives market. *Journal of Economic Dynamics and Control 133*, 104215.

Bargigli, L., G. Di Iasio, L. Infante, F. Lillo, and F. Pierobon (2015). The multiplex structure of interbank networks. *Quantitative Finance 15*(4), 673–691.

Barrat, A., M. Barthelemy, R. Pastor-Satorras, and A. Vespignani (2004). The architecture of complex weighted networks. *Proceedings of the national academy of sciences 101*(11), 3747–3752.

Brunnermeier, M. K., L. Clerc, Y. E. Omari, S. Gabrieli, S. Kern, C. Memmel, T. Peltonen, N. Podlich, M. Scheicher, and G. Vuillemey (2013). Assessing contagion risks from the cds market. *ESRB: Occasional Paper Series* (2013/04).

Cetina, J., M. Paddrik, and S. Rajan (2018). Stressed to the core: Counterparty concentrations and systemic losses in cds markets. *Journal of Financial Stability 35*, 38–52.

Chinazzi, M., G. Fagiolo, J. A. Reyes, and S. Schiavo (2013). Post-mortem examination of the international financial network. *Journal of Economic Dynamics and Control 37*(8), 1692–1713.

Clauset, A., M. E. Newman, and C. Moore (2004). Finding community structure in very large networks. *Physical review E 70*(6), 066111.

Clerc, L., S. Gabrieli, S. Kern, and Y. El Omari (2014). Monitoring the european cds market through networks: Implications for contagion risks. *Banque de France Working Paper Series* (477).

Cohen, R. and S. Havlin (2003). Scale-free networks are ultrasmall. *Physical review letters 90*(5), 058701.

Doyle, J. C., D. L. Alderson, L. Li, S. Low, M. Roughan, S. Shalunov, R. Tanaka, and W. Willinger (2005). The "robust yet fragile" nature of the internet. *Proceedings of the National Academy of Sciences 102*(41), 14497–14502.

Duffie, D., M. Scheicher, and G. Vuillemey (2015). Central clearing and collateral demand. *Journal of Financial Economics 116*(2), 237–256.

Duffie, D. and H. Zhu (2011). Does a central clearing counterparty reduce counterparty risk? *The Review of Asset Pricing Studies 1*(1), 74–95.

Erdős, P., A. Rényi, et al. (1960). On the evolution of random graphs. *Publ. Math. Inst. Hung. Acad. Sci 5*(1), 17–60.

Fricke, D. and T. Lux (2015). On the distribution of links in the interbank network: evidence from the e-mid overnight money market. *Empirical Economics 49*(4), 1463–1495.

Gabaix, X. and R. Ibragimov (2011). Rank- 1/2: a simple way to improve the ols estimation of tail exponents. *Journal of Business & Economic Statistics 29*(1), 24–39.

Gai, P. and S. Kapadia (2010). Contagion in financial networks. *Proceedings of the Royal Society A: Mathematical, Physical and Engineering Sciences 466*(2120), 2401–2423.

Heath, A., G. Kelly, M. Manning, S. Markose, and A. R. Shaghaghi (2016). Ccps and network stability in otc derivatives markets. *Journal of financial stability 27*, 217–233.

Kahros, A., A. Pioli, T. Carraro, M. Gravanis, and F. Vacirca (2021). A descriptive analysis of the client clearing network in the european derivatives landscape. *Journal of Financial Market Infrastructures 9*(1).

Lux, T. (2015). Emergence of a core-periphery structure in a simple dynamic model of the interbank market. *Journal of Economic Dynamics and Control 52*, A11–A23.

Mantegna, R. N. (1999). Hierarchical structure in financial markets. *The European Physical Journal B-Condensed Matter and Complex Systems 11*(1), 193–197.

Markose, S., S. Giansante, and A. R. Shaghaghi (2012). 'too interconnected to fail'financial network of us cds market: Topological fragility and systemic risk. *Journal of Economic Behavior & Organization 83*(3), 627–646.

McDonald, R. and A. Paulson (2015). Aig in hindsight. *Journal of Economic Perspectives 29*(2), 81–106.

Meilă, M. (2007). Comparing clusterings—an information based distance. *Journal of multivariate analysis 98*(5), 873–895.

Newman, M. E. (2002). Assortative mixing in networks. *Physical review letters 89*(20), 208701.

Newman, M. E. (2006). Modularity and community structure in networks. *Proceedings of the national academy of sciences 103*(23), 8577–8582.

Onnela, J.-P., A. Chakraborti, K. Kaski, J. Kertesz, and A. Kanto (2003). Dynamics of market correlations: Taxonomy and portfolio analysis. *Physical Review E 68*(5), 056110.

Peltonen, T. A., M. Scheicher, and G. Vuillemey (2014). The network structure of the cds market and its determinants. *Journal of Financial Stability 13*, 118–133.

Peralta, G. and A. Zareei (2016). A network approach to portfolio selection. *Journal of Empirical Finance 38*, 157–180.

Raffinot, T. (2017). Hierarchical clustering-based asset allocation. *The Journal of Portfolio Management 44*(2), 89–99.

Rosati, S. and F. Vacirca (2019). Interdependencies in the euro area derivatives clearing network: a multi-layer network approach. *ECB Working Paper Series* (2342).

Rosvall, M. and C. T. Bergstrom (2008). Maps of random walks on complex networks reveal community structure. *Proceedings of the national academy of sciences 105*(4), 1118–1123.

Rytgaard, M. (1990). Estimation in the pareto distribution. *ASTIN Bulletin: The Journal of the IAA 20*(2), 201–216.

Silva, T. C., S. R. S. de Souza, and B. M. Tabak (2016). Network structure analysis of the brazilian interbank market. *Emerging Markets Review 26*, 130–152.

Squartini, T., I. Van Lelyveld, and D. Garlaschelli (2013). Early-warning signals of topological collapse in interbank networks. *Scientific reports 3*(1), 1–9.

Tan, F., Y. Xia, and Z. Wei (2015). Robust-yet-fragile nature of interdependent networks. *Physical Review E 91*(5), 052809.

Tonzer, L. (2015). Cross-border interbank networks, banking risk and contagion. *Journal of Financial Stability 18*, 19–32.

Tumminello, M., F. Lillo, and R. N. Mantegna (2010). Correlation, hierarchies, and networks in financial markets. *Journal of economic behavior & organization 75*(1), 40–58.

Zhang, D., M. Hu, and Q. Ji (2020). Financial markets under the global pandemic of covid-19. *Finance research letters 36*, 101528.

Acknowledgements

I gratefully acknowledge Linda Rousová, Dilyara Salakhova, Tiziano Squartini and Martin Scheicher for the valuable comments and suggestions.
The views expressed in this paper are only mine and do not necessarily reflect those of the European Central Bank. All the errors are my own.

Sebastiano Michele Zema
European Central Bank, Frankfurt am Main, Germany; email: Sebastiano_Michele.Zema@ecb.europa.eu

PDF ISBN 978-92-899-5308-5 ISSN 1725-2806 doi:10.2866/808285 QB-AR-22-086-EN-N